

Exogenous fatty acids inhibit fatty acid synthesis by competing with endogenously generated substrates for phospholipid synthesis in *Escherichia coli*

van den Berg, Stefan Pieter Hendrik; Zoumaro-Djayoon, Adja; Yang, Flora; Bokinsky, Gregory

DOI

[10.1002/1873-3468.15092](https://doi.org/10.1002/1873-3468.15092)

Publication date

2025

Document Version

Final published version

Published in

FEBS Letters

Citation (APA)

van den Berg, S. P. H., Zoumaro-Djayoon, A., Yang, F., & Bokinsky, G. (2025). Exogenous fatty acids inhibit fatty acid synthesis by competing with endogenously generated substrates for phospholipid synthesis in *Escherichia coli*. *FEBS Letters*, 599(5), 667-681. <https://doi.org/10.1002/1873-3468.15092>

Important note

To cite this publication, please use the final published version (if applicable).
Please check the document version above.

Copyright



Other than for strictly personal use, it is not permitted to download, forward or distribute the text or part of it, without the consent of the author(s) and/or copyright holder(s), unless the work is under an open content license such as Creative Commons.

Takedown policy

Please contact us and provide details if you believe this document breaches copyrights.
We will remove access to the work immediately and investigate your claim.

RESEARCH ARTICLE

Exogenous fatty acids inhibit fatty acid synthesis by competing with endogenously generated substrates for phospholipid synthesis in *Escherichia coli*

Stefan Pieter Hendrik van den Berg , Adja Zoumaro-Djajoon , Flora Yang and Gregory Bokinsky 

Department of Bionanoscience, Kavli Institute of Nanoscience, Delft University of Technology, Delft, The Netherlands

Correspondence

Gregory Bokinsky, van der Maasweg 9, Building 58, room F1.270, Delft 2629HZ, The Netherlands.

Tel: +31 15 2785552

E-mail: g.e.bokinsky@tudelft.nl

Present address

Department of Immunopathology, Sanquin Research Amsterdam, Amsterdam, The Netherlands

(Received 1 November 2024, revised 29 November 2024, accepted 15 December 2024, available online 30 December 2024)

doi:10.1002/1873-3468.15092

Edited by Anne Kenworthy

Exogenous fatty acids are directly incorporated into bacterial membranes, heavily influencing cell envelope properties, antibiotic susceptibility, and bacterial ecology. Here, we quantify fatty acid biosynthesis metabolites and enzymes of the fatty acid synthesis pathway to determine how exogenous fatty acids inhibit fatty acid synthesis in *Escherichia coli*. We find that acyl-CoA synthesized from exogenous fatty acids rapidly increases concentrations of long-chain acyl-acyl carrier protein (acyl-ACP), which inhibits fatty acid synthesis initiation. Accumulation of long-chain acyl-ACP is caused by competition with acyl-CoA for phospholipid synthesis enzymes. Furthermore, we find that transcriptional regulation rebalances saturated and unsaturated acyl-ACP while maintaining overall expression levels of fatty acid synthesis enzymes. Rapid feedback inhibition of fatty acid synthesis by exogenous fatty acids thus allows *E. coli* to benefit from exogenous fatty acids while maintaining fatty acid synthesis capacity. We hypothesize that this indirect feedback mechanism is ubiquitous across bacterial species.

Keywords: acyl carrier protein; exogenous fatty acids; fatty acid synthesis; homeoviscous adaptation; post-translational regulation

The synthesis of lipids for membrane biogenesis consumes considerable amounts of energy and metabolites. Microorganisms avoid this cost whenever possible by incorporating exogenous fatty acids directly into the cellular membrane [1]. Exogenous fatty acids exert profound effects on bacterial physiology and ecology and are particularly relevant to infectious disease. In pathogenic bacteria, exogenous fatty acids can facilitate or impede cold resistance [2,3], influence biofilm formation, and increase membrane permeability and antibiotic susceptibility [4,5]. Recently, host-derived fatty acids were found to support healthy microbiota within the female genital tract

and proved more effective than antibiotics *in vitro* at promoting strains that prevent bacterial vaginosis [6]. The mechanisms by which exogenous fatty acids affect physiology and trigger adaptations are incompletely understood.

Exogenous fatty acids enable some bacteria to evade fatty acid synthesis inhibitors [7], a finding that triggered an important debate about whether bacterial fatty acid synthesis is an appropriate target for clinical antibiotics. This debate intensified research into the effects of exogenous fatty acids on *de novo* fatty acid synthesis pathways. Early research with the model species *Escherichia coli* revealed that exogenous fatty acids

Abbreviations

ACC, acetyl-CoA carboxylase; ACP, acyl carrier protein; LCMS, liquid chromatography coupled with mass spectrometry; LPA, lysophosphatidic acid; MOPS, 3-(morpholine-4-yl)propane-1-sulfonic acid; PA, phosphatidic acid; PE, phosphatidylethanolamine; PG, phosphatidylglycerol; ppGpp, guanosine tetraphosphate; PS, phosphatidylserine.

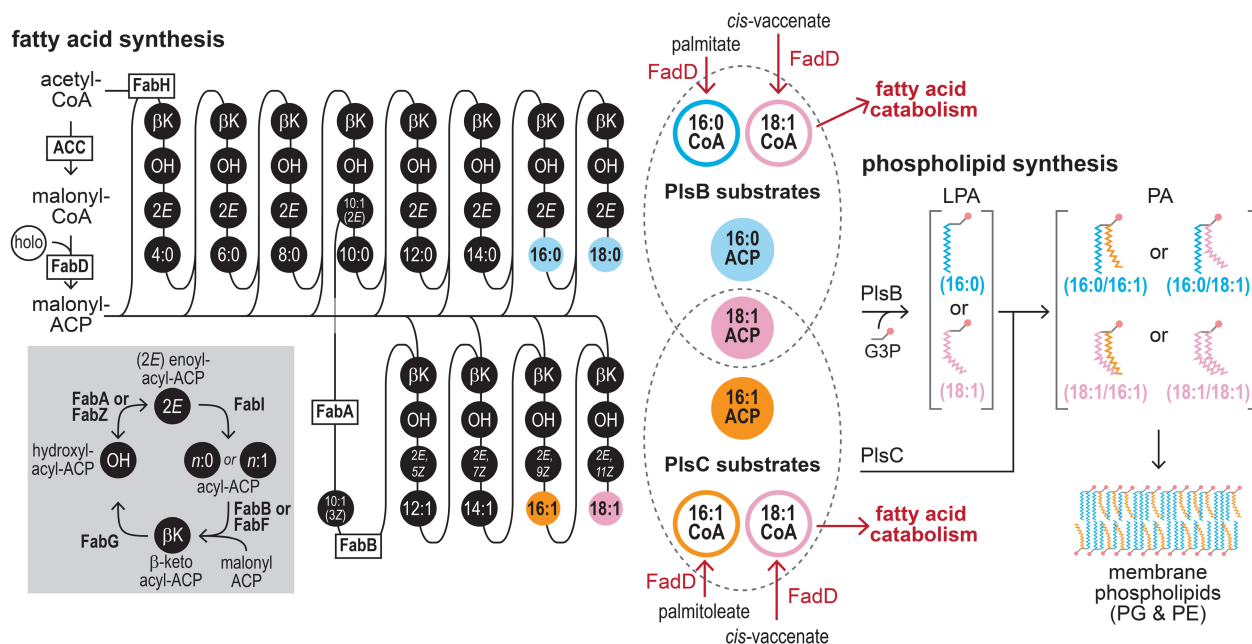


Fig. 1. The convergence of the fatty acid synthesis, fatty acid catabolism, and phospholipid synthesis pathways in *E. coli*. Fatty acids are synthesized by repeated cycles of elongation, dehydration, and reduction of acyl-ACP thioesters that ultimately yield long-chain fatty acyl-ACP. The *E. coli* pathway splits into saturated and unsaturated branches at the 10-carbon acyl-ACP intermediate C10:1(2E) ACP. FabA reversibly isomerizes (C10:1(2E)) with the precursor of the unsaturated pathway (C10:1(3Z) ACP). These precursors are irreversibly committed to the saturated and unsaturated branches by FabI and FabB, respectively. Phospholipid synthesis enzymes PlsB and PlsC use long-chain acyl-ACP products of fatty acid synthesis and acyl-CoA intermediates of fatty acid catabolism of appropriate length. PlsB initiates phospholipid synthesis by transferring acyl chains from preferred ACP or CoA substrates (16:0 or 18:1) to the *sn*-1 position of glycerol-3-phosphate (G3P), producing lysophosphatidic acid (LPA). PlsC transfers acyl groups from its preferred ACP or CoA substrates (16:1 or 18:1) to the *sn*-2 position of LPA, generating phosphatidic acid (PA). The relative proportions of acyl chains at *sn*-1 and *sn*-2 positions are determined by the corresponding proportion of acyl thioester substrates in the PlsB and PlsC substrate pools. Note that the substrate preferences of PlsB and PlsC are not absolute: PlsB incorporates a small amount of 16:1 acyl chains at *sn*-1 [28], while PlsC incorporates a small amount of 16:0 acyl chains at *sn*-2. PA is further converted via phospholipid headgroup addition and modification reactions to produce membrane phospholipids phosphatidylglycerol (PG) and phosphatidylethanolamine (PE).

inhibit *de novo* synthesis [8,9], although the mechanism remained unclear. In members of the Lactobacillales family (which includes pathogens such as *Enterococcus faecalis* and *Streptococcus pneumoniae*), exogenous fatty acids repress expression of the fatty acid synthesis pathway via the FabT transcriptional repressor protein [10–13]. The ability of *S. pneumoniae* to inhibit *de novo* synthesis when supplied with exogenous fatty acids allows the bacteria to resist fatty acid synthesis inhibitors [14], although whether this trait is enabled entirely by transcriptional regulation is unknown. However, very few species are able to completely replace fatty acid synthesis with exogenous fatty acids [1,15]. In many organisms, fatty acid synthesis is needed to supply precursors for essential membrane components such as lipopolysaccharides or branched-chain fatty acids. Furthermore, as incorporating exogenous fatty acids impacts membrane lipid composition, endogenous fatty acid synthesis pathways must adapt

to maintain membrane properties such as fluidity. This response is a form of homeoviscous adaptation and is similar to the adaptation of membrane composition to temperature [16].

In *Escherichia coli*, long-chain fatty acids are imported via the membrane channel FadL [17,18] and activated by the long-chain fatty acid-CoA ligase enzyme FadD [19]. A fraction of the acyl-CoA pool is then catabolized into acetyl-CoA by the fatty acid degradation pathway, while acyl-CoA of appropriate length are incorporated into phospholipids by the glycerol-3-phosphate acyl transferase PlsB and the lysophosphatidic acid acyl transferase PlsC (Fig. 1). Saturated and unsaturated long-chain fatty acids are also produced by the *E. coli* type II fatty acid synthesis pathway in the form of fatty acyl thioesters attached to an acyl carrier protein (acyl-ACP), which are also substrates for PlsB and PlsC. The ability of PlsB and PlsC to use both acyl-ACP and acyl-CoA as

Table 1. Primers used for constructing and confirming Δ fadD strain.

GB201127-fadDKO.f1	GGTTGCGATGACGACGAACACGCATTTTAGAGGTGAAGAA gtgtaggctggagctgcttc
GB201127-fadDKO.f2	TGATGAGTTAATATATGTTAACGGCATGTATATCATTTGGGGTTGCGATGACGACGAAC
GB201127-fadDKO.r1	CGAAACTCCACCAGCTTCGGTACTTTGTATCCCGTGAatgggaattagccatgggtcc
GB201127-fadDKO.r2	GTCGCAAAATTTTCCGACGTTAGATTTCGGTAACTCATCACGAAACTCCACCAGCTTCG
GB201201-fadDKO.fseq	CGTTGGGTAATTATCAAGCTGG
GB201201-fadDKO.rseq	GCGCTTCGTCACGTAATTCTC

phospholipid precursors places *de novo*-synthesized fatty acids in a common substrate pool with CoA-activated exogenous fatty acids. As a consequence, acyl-CoA substrates derived from exogenous fatty acids compete against acyl-ACP for incorporation into phospholipids [20]. The *E. coli* transcriptional response to exogenous fatty acids is directed by two transcriptional regulators, FadR and FabR. FadR, which is activated by long-chain acyl-CoA, primarily controls expression of the fatty acid degradation pathway [21] and influences expression of several fatty acid synthesis genes [22]. The transcriptional regulator FabR controls expression of the fatty acid synthesis enzymes FabA and FabB, which allocate flux between the saturated and unsaturated pathways [23,24] (Fig. 1).

While transcriptional regulation contributes to balancing the ratio of saturated and unsaturated fatty acids, fatty acid metabolism is also regulated via post-translational mechanisms such as classical feedback inhibition. The total flux passing through the fatty acid synthesis pathway is regulated by long-chain acyl-ACP, which inhibit acetyl-CoA carboxylase (ACC) [25] (Fig. 1). Concentrations of long-chain acyl-ACP (and thus ACC activity) are determined by PlsB activity, which is itself allosterically regulated to coordinate phospholipid synthesis with growth [26]. Furthermore, homeoviscous adaptation to temperature shocks is initiated by a post-translational response that rapidly increases the proportion of saturated or unsaturated fatty acids [27,28]. Exogenous fatty acids may also affect fatty acid synthesis through post-translational mechanisms. In particular, the enoyl-ACP reductase enzyme FabI was reported to be inhibited by acyl-CoA [29], a finding that is often proposed to explain the effects of exogenous fatty acids on membrane assembly and homeostasis [30,31]. How acyl-CoA uses allosteric and transcriptional mechanisms to regulate fatty acid synthesis is unclear.

Here, we describe the mechanism by which exogenous fatty acids inhibit fatty acid synthesis in *E. coli*. We find that acyl-CoA causes accumulation of long-chain acyl-ACP due to competition for acyltransferase enzymes PlsB and PlsC. Acyl-ACP

accumulation in turn inhibits fatty acid synthesis initiation by ACC. We find no evidence that acyl-CoA inhibits FabI. A mathematical model simulating substrate competition between ACP and CoA substrates closely recapitulates our experimental results. Our findings demonstrate how the cellular demand for phospholipid synthesis retains control over fatty acid synthesis flux regardless of the availability of exogenous fatty acids.

Methods

Strains, chemicals, and growth conditions

Escherichia coli K-12 strain NCM3722 (CGSC #12355) was used for all experiments. NCM3722 Δ fadD was constructed using lambda-red recombination [42] with primers listed in Table 1. Cultures were prepared in Erlenmeyer flasks with 0.2% w/vol glycerol in MOPS minimal medium [43]. Flasks were maintained at 37 °C by submersion in a Grant Instruments Sub Aqua Pro water bath and stirred (1200 rpm) using a magnetic stir bar (20 mm) coupled to a stir plate (2mag MIXdrive 1 Eco and MIXcontrol 20). Growth was monitored with optical density measurements (Ultrospec 10 Cell Density Meter; GE Healthcare, Chicago, IL, USA). Fatty acids (40 mM) were neutralized to pH 7 using NaOH and solubilized with 26% Tergitol NP-40 before dilution in culture medium. Fatty acids were obtained from Sigma-Aldrich: palmitic acid (P0500), palmitoleic acid (P9417), and *cis*-vaccenic acid (V0384). Unsaturated fatty acids were stored at −20 °C and prepared as solutions immediately before use.

Culture sampling for LCMS analysis

Samples (usually 1 mL) for all analysis modalities were rapidly removed from cultures and quenched by pipetting directly into ice-cold 10% trichloroacetic acid (TCA) to 2% final TCA concentration, pelleted, and stored at −80 °C until processing for analysis.

LCMS quantification and analysis

LCMS methods are fully described in reference [26]. LCMS was performed using Agilent LCMS (binary pump

(G1312B), autosampler (G7167A), temperature-controlled column compartment (G1316A), and triple quadrupole (QQQ) mass spectrometer (G6460C) equipped with a standard ESI source) all operated using MassHunter (version 7.0). Mass spectrometer set in dynamic MRM mode using transitions generated *in silico* by a script written in Python using RDKit library. Transitions for targeted proteomics assays were developed using Skyline [44]. LCMS data were further processed in Skyline versions 4.x using an *in silico* generated transition list for targets and corresponding internal standards.

Acyl-ACP quantification

Sample pellets were lysed by suspending quenched pellets in a buffered urea solution (10 mL of 50 mM potassium phosphate buffer, pH 7.2, 6 M urea, 10 mM N-ethylmaleimide, 5 mM EDTA and 1 mM ascorbic acid) with ^{15}N -labeled internal standards (generated using $\text{U-}^{15}\text{N}$ *E. coli* whole cell extracts from MOPS minimal medium cultures with $^{15}\text{NH}_4\text{Cl}$ as the sole nitrogen source) and proteins precipitated according to [26]. Protein pellet was resolubilized in 10 μL digestion buffer (4% 2-octylglucoside, 25 mM potassium phosphate pH 7.2) and digested initiated by adding 10 μL of 0.1 $\text{mg}\cdot\text{mL}^{-1}$ GluC protease (Promega, Madison, WI, USA). Digestion continued overnight at 37 °C. After quenching with 5 μL MeOH, samples were centrifuged and 10 μL injected into LC/MS. Separation was performed on 2.1 mm \times 50 mm 1.7 μm CSH C-18 column (Waters, Milford, MA, USA) held at 80 °C using a binary gradient: 15% B, 3 min ramp to 25%, 9 min increase to 95%, and 1 min hold at 95% B before 3 min re-equilibration at starting conditions (A: 25 mM formic acid, B: 50 mM formic acid) at a flow rate of 0.6 $\text{mL}\cdot\text{min}^{-1}$. MS transitions for both ^{14}N and ^{15}N acyl-ACP were developed as described in [32] and [26].

Phospholipid quantification

TCA-quenched sample pellets were resuspended in 150 μL of MeOH, 250 μL of $\text{U-}^{13}\text{C}$ *E. coli* phospholipid extract, and 250 μL *m*-tert-butyl ether (MTBE) and subsequently vortexed and sonicated in a water bath. 125 μL of 15 mM citric acid/20 mM dipotassium phosphate buffer was added to homogenized pellets and vortexed. Liquid phases were separated by centrifugation for 10 min at 20 000 *g*. 450 μL of the upper phase was moved to a new tube and dried in a vacuum centrifuge. Dried lipids were resuspended in 10 μL 65 : 30 : 5 (v/v/v) isopropanol/acetonitrile/ H_2O supplemented with 10 mM acetylacetone. After addition of 5 μL H_2O , 5 μL of resulting mixture was injected into the LC/MS system. Separation was performed on 2.1 mm \times 50 mm 1.7 μm CSH C-18 column (Waters) at 60 °C with a flow rate of 0.6 $\text{mL}\cdot\text{min}^{-1}$ using the following binary gradient: 25% B, ramp to 56% B in 6 min followed

by linear increase to 80% B in 6 min, 2 min hold at 100% B and 3 min re-equilibration (A: 0.05% NH_4OH in water, B: 0.05% NH_4OH in 80% isopropanol 20% ACN).

Targeted protein quantification

TCA-quenched sample pellets were resuspended in 1 mL of 50 mM potassium phosphate buffer, pH 7.2 and 6 M urea that had been premixed with $\text{U-}^{15}\text{N}$ -labeled *E. coli* internal standards. After precipitation in chloroform/methanol, protein pellets were resuspended in 10 μL of digestion buffer (4% 2-octylglucoside in 25 mM Tris buffer pH 8.1, 1 mM CaCl_2 , 5 mM TCEP). Cysteines were alkylated by adding 3 μL of 50 mM iodoacetamide followed by 15 min of incubation. Digestion initiated by addition of 10 μL of 0.2 $\text{mg}\cdot\text{mL}^{-1}$ Trypsin Gold (Promega). After overnight digestion at 37 °C, 10 μL of digestion reaction was injected in LCMS system and separation performed on 2.1 mm \times 50 mm 1.7 μm CSH C-18 column (Waters) held at 40 °C using a binary gradient: 2% B, 20 min ramp to 25% B, 4 min increase to 40% B, 0.5 min ramp to 80%, and 1 min hold at 80% B before 3 min re-equilibration at starting conditions (A: 25 mM formic acid, B: 50 mM formic acid) at a flow rate of 0.5 $\text{mL}\cdot\text{min}^{-1}$. Analysis of kinetic data revealed that addition of Tergitol NP-40 (carrier to solubilize fatty acids) affected detected protein concentrations. All protein quantities were therefore normalized to the abundance of elongation factor TufA to account for effects of Tergitol.

Mathematical modeling

The mathematical model was constructed using COPASI version 4.39 (build 272). Full details of the model are included in the Supplementary Information.

Results

Acyl-CoA from exogenous fatty acids immediately inhibits *de novo* fatty acid synthesis

To characterize how the *E. coli* fatty acid pathway responds to the uptake and incorporation of exogenous fatty acids, we quantified acyl-ACP intermediates before and after feeding fatty acids to an exponential-phase culture. Cultures of *E. coli* NCM3722 were prepared at 37 °C in defined minimal medium (MOPS/0.2% glycerol). When culture density reached an optical density of ~ 0.4 , palmitate (C16:0 fatty acid, solubilized with Tergitol NP-40 as a carrier) was added to achieve final concentration of 0.8 mM. Samples for analysis by liquid chromatography coupled with mass spectrometry (LCMS) were removed from the culture immediately before and after

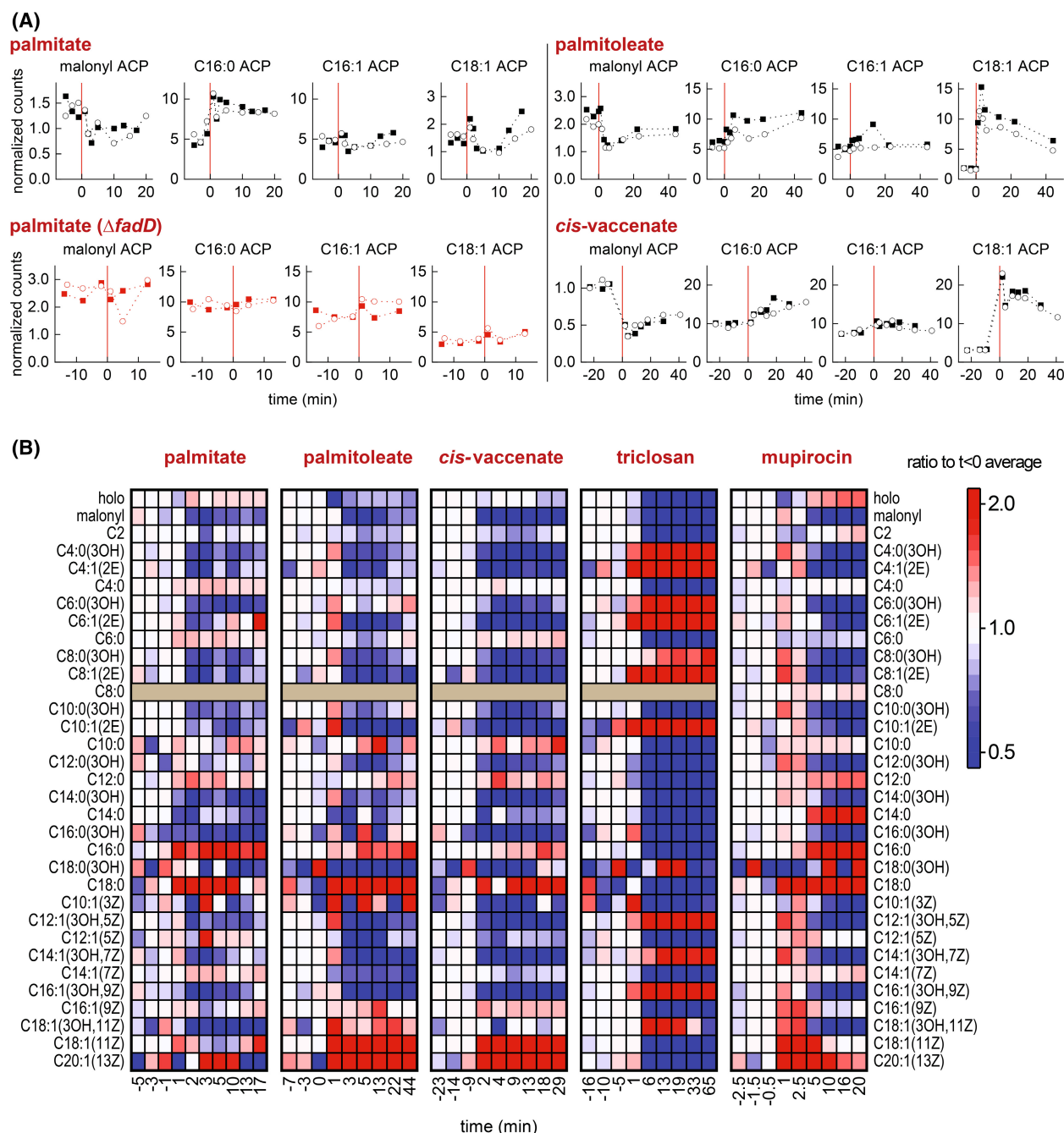


Fig. 2. Acyl-ACP pools respond immediately to acyl-CoA synthesized from exogenous fatty acids added to the growth medium. (A) Concentrations of acyl-ACP quantified before and after addition of indicated exogenous fatty acid (added at 0 min, indicated with vertical red lines). All counts normalized to counts obtained from a nonacylated ACP peptide (LVMALE). Responses of two biological replicates in each condition are displayed; each point represents a single measurement. (B) Heat map representation of all acyl-ACP pools following acyl-CoA synthesis, triclosan addition, and addition of the isoleucine-tRNA ligase inhibitor mupirocin [46], which triggers ppGpp synthesis. All values normalized to average of three measurements before treatments. Data are representative of two biological replicates. Triclosan data from [28] and mupirocin data from [26]. Measurements of C8:0 ACP lost in some datasets due to recording error.

palmitate feeding [32]. Surprisingly, concentrations of key acyl-ACP responded within 1 min after palmitate feeding (Fig. 2A). The fatty acid initiation and

elongation substrate malonyl-ACP decreased by nearly 50%, suggesting inhibited synthesis of malonyl-CoA by ACC. Interestingly, palmitate feeding immediately

increased the PlsB substrate C16:0 ACP by ~2-fold while unsaturated long-chain acyl-ACP C16:1 and C18:1 remained relatively unchanged. Hydroxyl-acyl-ACP and 2(*E*)-enoyl-acyl-ACP species, whose concentrations tightly correlate with fatty acid synthesis flux during steady-state growth [26], also decreased by approximately 50% (Fig. 2B). Palmitate did not affect acyl-ACP pools of a strain lacking FadD (NCM3722 Δ fadD), consistent with the effects observed being driven by C16:0 CoA synthesized from exogenous palmitate (Fig. 2A).

We next tested the effects of adding unsaturated fatty acids palmitoleate (C16:1(9Z)) and *cis*-vaccenate (C18:1(11Z)) on the acyl-ACP pools. Similar to palmitate, addition of both fatty acids to 0.8 mM immediately decreased malonyl-ACP by approximately 50% (Fig. 2A) and decreased concentrations of hydroxyl-acyl-ACP and 2(*E*)-enoyl-acyl-ACP by ~50% (Fig. 2B), again consistent with fatty acid synthesis inhibition. However, unlike palmitate, both unsaturated fatty acids increased C18:1 ACP by ~5-fold and triggered a relatively small increase in C16:0 ACP. The accumulation of long-chain acyl-ACP and simultaneous reduction of malonyl-ACP and acyl-ACP intermediates that correlate with fatty acid flux strongly suggests that acyl-CoA inhibits fatty acid synthesis by triggering feedback inhibition of ACC by long-chain acyl-ACP. Interestingly, exogenous fatty acids increased the low-abundance C18:0 and C20:1 ACP by severalfold (Fig. 2B). This is consistent with an increase in the rate of acyl-ACP elongation relative to the rate of acyl-ACP consumption by the acyltransferases PlsB and PlsC.

Fatty acid synthesis inhibition by acyl-CoA does not resemble inhibition by the FabI inhibitor triclosan

The response of the acyl-ACP pools to acyl-CoA is far too rapid (~1 min) to be mediated by transcriptional regulation. Therefore, acyl-CoA must inhibit fatty acid synthesis via direct interactions with enzymes within either the fatty acid or phospholipid synthesis pathways. C16:0 CoA has been proposed to inhibit fatty acid synthesis by inhibiting the enoyl-acyl-ACP reductase FabI [29]. This conclusion is based upon *in vitro* experiments which used enoyl-acyl-CoA as a substitute for the actual FabI substrate enoyl-acyl-ACP. However, the effects of acyl-CoA on acyl-ACP pools that we observe do not resemble the effects of the FabI inhibitor triclosan [33]. In contrast with the acyl-CoA response, triclosan entirely depleted all long-chain acyl-ACP (Fig. 2A). While triclosan also depletes

malonyl-ACP, concentrations of hydroxyl-acyl-ACP and 2(*E*)-enoyl-acyl-ACP dramatically increase by several fold, a response opposite to the 2-fold depletion of hydroxyl-acyl-ACP and 2(*E*)-enoyl-acyl-ACP caused by acyl-CoA (Fig. 2B). Furthermore, all acyl-ACP products of FabI decrease, a response not triggered by acyl-CoA. The accumulation of FabI substrates ((2*E*)-enoyl-acyl-ACP, which rapidly equilibrates with hydroxyl-acyl-ACP) and depletion of FabI products is consistent with FabI inhibition. Finally, triclosan depletes holo-ACP, while acyl-CoA does not consistently affect holo-ACP abundance. Overall, the stark differences between the acyl-ACP pool dynamics following acyl-CoA synthesis and triclosan inhibition indicate that acyl-CoA does not suppress fatty acid synthesis *in vivo* by inhibiting FabI.

Acyl-CoA synthesized from exogenous fatty acids rapidly alters lipid composition of phospholipid intermediates

The effects of acyl-CoA on acyl-ACP pools, in particular the rapid depletion of malonyl-ACP and hydroxyl-acyl-ACP species, resemble the effects of phospholipid synthesis arrest by the alarmone guanosine tetraphosphate (ppGpp) [26] (Fig. 2B). After activating ppGpp synthesis by addition of mupirocin to the growth medium, inhibition of phospholipid synthesis by ppGpp triggers accumulation of both saturated and unsaturated long-chain acyl-ACP. Long-chain acyl-ACP inhibits synthesis of malonyl-CoA by ACC, which in turn decreases malonyl-ACP concentrations, and thus, the elongation reactions catalyzed by β -keto-acyl-ACP synthases FabH, FabB, and FabF. This is evident from decreased concentrations of malonyl-ACP as well as depletion of flux-sensitive intermediates hydroxyl-acyl-ACP and 2(*E*)-enoyl-acyl-ACP when ppGpp is elevated [26]. Furthermore, phospholipid synthesis inhibition by ppGpp also depletes the phospholipid synthesis intermediates PA and phosphatidylserine (PS). However, unlike phospholipid synthesis inhibition by ppGpp, acyl-CoA synthesized from exogenous fatty acids does not substantially deplete PA and PS (Fig. 3A). Instead, within 1–2 min of feeding, the acyl chain compositions of phospholipid synthesis intermediates immediately change (Fig. 3B). Specifically, palmitate slightly increases the fraction of PA bearing 16:0 acyl chains at *sn*-1, consistent with greater incorporation of C16:0 fatty acid by PlsB from C16:0 CoA. Strikingly, palmitate also increases the proportion of phospholipids with C16:0 at *sn*-2, consistent with utilization of C16:0 CoA by PlsC. These changes in the composition of the PA intermediate pool

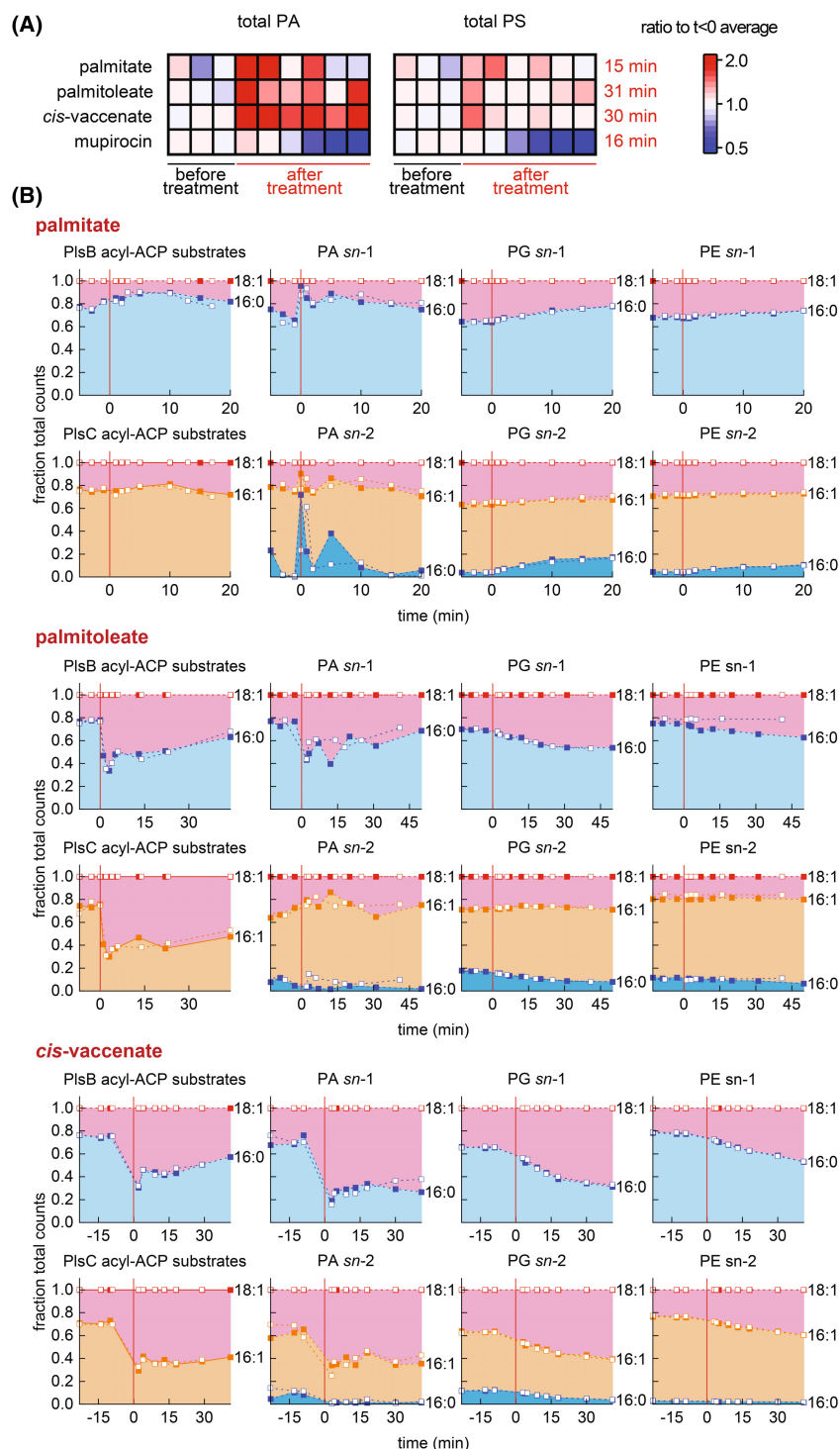


Fig. 3. Phospholipid intermediate and membrane phospholipid pools respond immediately to acyl-CoA synthesis. (A) Relative abundance of PA and phosphatidylserine (PS) immediately following exogenous fatty acid feeding compared with phospholipid synthesis inhibition by ppGpp (ppGpp synthesis triggered by mupirocin). All values normalized to average of three measurements before treatments. Data are representative of two biological replicates. Mupirocin data from [26]. Values on right axis indicate time of final measurement shown. (B) Comparison of PlsB and PlsC substrate pools with composition of PA and membrane phospholipids PG and PE before and after addition of exogenous fatty acids. Areas represent fraction of total LCMS counts for phospholipid species bearing indicated acyl chains at either the *sn*-1 or *sn*-2 positions. All kinetic series obtained from 2 independent experiments, which are distinguished by closed and open symbols.

propagate over time to alter the lipid composition of the membrane phospholipids PG and PE (Fig. 3B).

Addition of the unsaturated fatty acid palmitoleate also rapidly changed the composition of the PA intermediate pool. Although C16:1 CoA is not expected to significantly contribute to the PlsB substrate pool, palmitoleate immediately increased the proportion of C18:1 *sn*-1 PA (Fig. 3B). This is due to the sudden increase in C18:1 ACP caused by C16:1 CoA. Similarly, palmitoleate rapidly perturbed the composition of the PlsC acyl-ACP substrate pool, with C18:1 ACP becoming the predominant ACP thioester. However, the proportion of lipids incorporated at PA *sn*-2 did not match the proportions represented within the PlsC acyl-ACP substrate pool, reflecting the presence of C16:1 CoA countering the increased concentration of C18:1 ACP. *Cis*-vaccenate feeding dramatically increased the proportion of C18:1 ACP within the acyl-ACP pools of both PlsB and PlsC and immediately changed the lipid composition at both the *sn*-1 and *sn*-2 positions of PA, which propagated to the composition of membrane phospholipids PG and PE (Fig. 3B). These results indicate that exogenous fatty acids alter the lipid composition both directly (through use of acyl-CoA substrates by PlsB and PlsC) and indirectly (by changing the composition of the long-chain acyl-ACP pool). We note that chain shortening by β -oxidation of C18:1 CoA generates the PlsC substrate C16:1 CoA, which is likely to further decrease consumption of the acyl-ACP pool.

Importantly, the specific acyl-ACP product that accumulates corresponds to the identity of the acyl-CoA generated from the exogenous fatty acid: palmitate causes accumulation of saturated acyl-ACP, whereas unsaturated exogenous fatty acids cause accumulation of unsaturated acyl-ACP. This is likely due to the substrate preferences of the acyltransferase enzymes. This effect further increases the incorporation of saturated or unsaturated fatty acids from the acyl-ACP pools into the membrane, thus amplifying the influence of acyl-CoA on the balance of saturated/unsaturated membrane lipids.

A mathematical model simulating competition between acyl-ACP and acyl-CoA for PlsB and PlsC reproduces acyl-ACP perturbations and fatty acid synthesis inhibition

While it is clear how acyl-CoA is able to rapidly change the lipid composition of newly synthesized phospholipids, it is less obvious how acyl-CoA triggers acyl-ACP accumulation and fatty acid synthesis inhibition. The strong and rapid effects of acyl-CoA on the

lipids incorporated into phospholipids indicate that acyl-ACP and acyl-CoA compete for PlsB and PlsC active sites, as previously observed [20]. This competition in turn suggests a mechanism by which acyl-CoA decreases malonyl-ACP concentrations and thereby attenuates fatty acid flux: as a competing substrate, acyl-CoA decreases acyl-ACP consumption by PlsB and PlsC, causing long-chain acyl-ACP to accumulate and inhibit malonyl-CoA synthesis by ACC. This is consistent with the decreased concentrations of malonyl-ACP and other flux-sensitive acyl-ACP (hydroxyl-acyl-ACP and (2*E*)-enoyl-acyl-ACP).

To test this notion, we constructed a mathematical model of the *E. coli* fatty acid and phospholipid synthesis pathways using the simulation software COPASI [34]. For simplicity, the simulated fatty acid synthesis pathway included only initiation and elongation steps. Fatty acid synthesis initiation reactions were combined to a single ACC-FabD reaction generating malonyl-ACP from holo-ACP and acetyl-CoA, followed by FabH condensing malonyl-ACP with acetyl-CoA (Fig. 4A). All subsequent elongation reactions were represented by a 'FabB' reaction modified to account for combined chain length preferences of β -keto-acyl-ACP synthases FabB and FabF [35]. The branch point between saturated and unsaturated pathways was simulated as two parallel reactions consuming C10:0 ACP as a common substrate. A term implementing feedback inhibition of the ACC-FabD reaction by the long-chain acyl-ACP pool was also included. All enzymatic reactions were simulated as one- or two-substrate reactions using Michaelis–Menten kinetics with the exception of the reactions catalyzed by PlsB and PlsC. To simulate substrate competition, the separate binding/unbinding and catalytic steps of acyl-ACP and acyl-CoA substrates with PlsB and PlsC were explicitly included (Fig. 4B), following the example of recent modeling work [36]. In order to maintain overall phospholipid flux at a fixed value despite the changing abundance of PlsB and PlsC substrates, a feedback inhibition term controlling PlsB activity based on total phospholipid content was included. Generation of acyl-CoA was simulated by a stepwise change in acyl-CoA concentration after the simulation had reached steady state. Further details of the simulation are included within the Supplementary Information.

Similar to our experimental observations, the simulated stepwise increase in C16:0 CoA (emulating palmitate feeding) immediately increased both C16:0 and C18:0 ACP and decreased malonyl-ACP (Fig. 4C). The increase in C16:0 ACP is the direct result of substrate competition between C16:0 ACP and C16:0 CoA, while the increase in C18:0 ACP results from increased

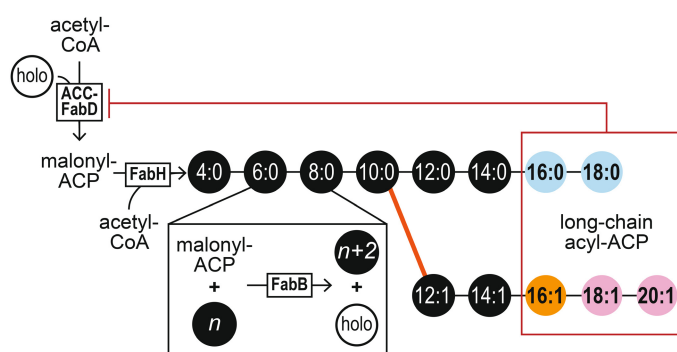
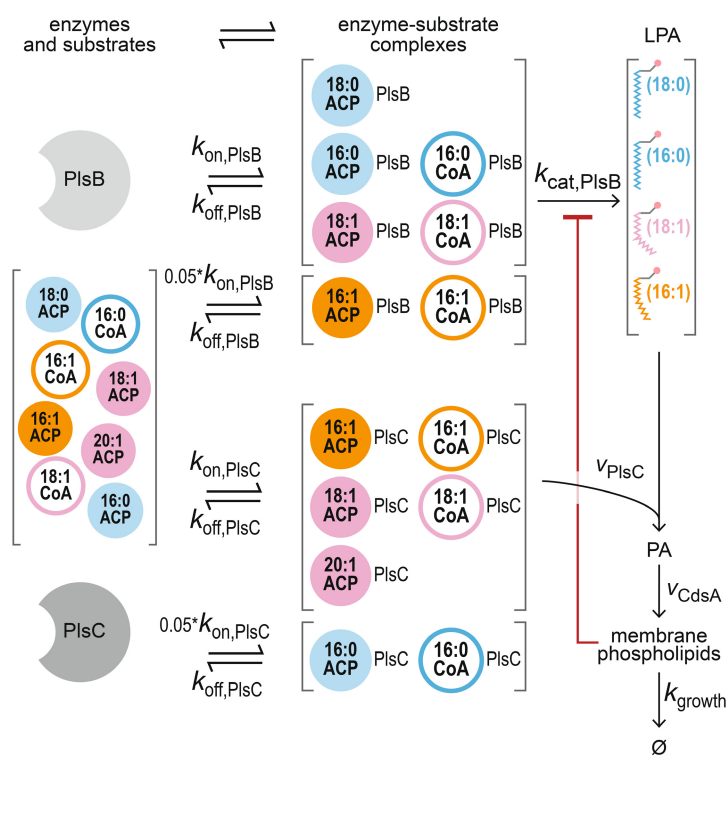
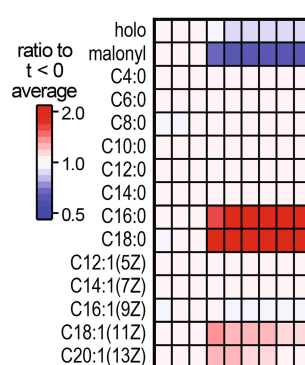
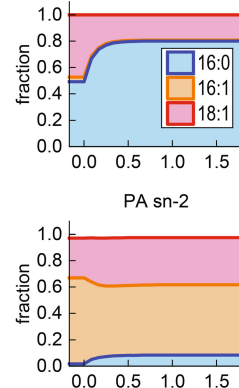
(A) fatty acid synthesis**(B) PlsB/PlsC substrate competition****(C)****(D)**

Fig. 4. A mathematical model of the fatty acid and phospholipid synthesis pathways that explicitly simulates substrate competition between acyl-CoA and acyl-ACP reproduces experimental results. (A, B) Diagram of the simplified fatty acid pathway (A) and substrate competition scheme (B) used in the simulation. Substrate preferences for PlsB (disfavoring C16:1 ACP and C16:1 CoA) and PlsC (disfavoring C16:0 ACP and C16:0 CoA) are implemented by decreasing the binding rates (k_{on}) for these substrates. (C, D) Simulation output for acyl-ACP pools (C) and phospholipid intermediate lipid compositions (D) after exogenous fatty acid feeding at 0 min. Detailed explanation of the model, including differential equations and parameters used, are included in the Supplementary Information.

abundance of substrate for the elongation reaction to 18:0 ACP. Furthermore, our model also reproduced the changing composition of the PA pool, with C16:0 increasing at *sn*-1 and *sn*-2 (Fig. 4D). Simulated production of C16:1 CoA (equivalent to palmitoleate feeding) also closely followed our experimental observations. C16:1 CoA increased long-chain unsaturated acyl-ACP and decreased malonyl-ACP. The increase in C18:1 ACP also increased the fraction of 18:1 *sn*-1 PA. However, just as in our observations, palmitoleate slightly decreased the 18:1 *sn*-2 PA pool, reflecting the incorporation of palmitoleate from C16:1 CoA by PlsC. Finally, simulated responses of the acyl-ACP pools to *cis*-vaccenate feeding also closely followed our experimental observations: both saturated and unsaturated long-chain acyl-ACP increased significantly while malonyl-ACP decreased. The increased proportions of 18:1 at both *sn*-1 and *sn*-2 PA after *cis*-vaccenate feeding also mirror our experimental observations.

The FabA/FabB ratio is adjusted to restore proportions of saturated and unsaturated acyl-ACP within the PlsB substrate pool

The changes in membrane composition induced by exogenous fatty acid incorporation affect biophysical properties of the phospholipid membrane such as membrane fluidity and thickness. To maintain the biophysical properties of its membrane, *E. coli* controls relative synthesis rates of saturated and unsaturated fatty acids by adjusting expression of the branch point enzymes FabA and FabB: decreasing the FabA/FabB ratio increases the production of unsaturated fatty acids, while increasing FabA/FabB increases the production of saturated fatty acids [24]. We quantified proteins of the fatty acid synthesis pathway using LCMS to determine the transcriptional response to exogenous fatty acids. After palmitate feeding, FabB steadily increased and reached final steady-state level after approximately 2 h. In contrast, FabA levels remained constant (Fig. 5A), causing the FabA/FabB

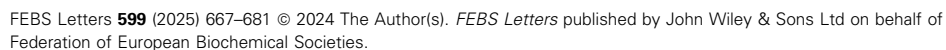
ratio to decrease (Fig. 5B). These changes were not observed in cultures treated with solubilizing carrier alone or in cultures of palmitate-fed Δ *fadD*. In contrast, addition of unsaturated fatty acids palmitoleate and *cis*-vaccenate decreased both FabA and FabB. After two generation periods, the FabA/FabB steady-state ratios increased slightly, consistent with the expected homeostatic response.

The changes in the FabA/FabB ratio adapt the abundance of long-chain acyl-ACP and the relative proportions within the PlsB and PlsC substrate pools (Fig. 5C). After two doublings in palmitate-supplemented medium, concentrations of unsaturated acyl-ACP increase by approximately 50%, whereas C16:0 ACP increases after two doublings in medium supplemented with either palmitoleate or *cis*-vaccenate. Surprisingly, despite these adaptations in the fatty acid synthesis pathway, the final steady-state fraction of C16:0 ACP within the PlsB substrate pool in all three fatty acid-supplemented conditions matched the ratio existing before fatty acid addition (~0.8). This suggests that the transcriptional response to exogenous fatty acids restores the C16:0/C18:1 ACP ratio existing prior to exogenous fatty acid feeding. We also quantified the remaining enzymes of the fatty acid synthesis pathway during steady-state growth in the presence of exogenous fatty acids. Interestingly, with the exception of FabA and FabB, all enzyme concentrations remained constant, as did the first three enzymes of phospholipid synthesis (PlsB, PlsC, CdsA) (Fig. 5D). This indicates that expression of the fatty acid synthesis pathway remains constant despite the availability of exogenous fatty acids. Thus, while transcriptional regulation adjusts the relative proportions of saturated and unsaturated acyl-ACP, it does not downregulate expression of the fatty acid synthesis pathway.

Discussion

The conversion of exogenous fatty acids to substrates for membrane synthesis inhibits endogenous fatty acid

Fig. 5. Transcriptional response of the fatty acid pathway to exogenous fatty acids. (A) Normalized response ($t < 0$ average = 1) of FabA and FabB concentrations after feeding of exogenous fatty acids compared with solubilizing carrier control. Data from two biological replicates displayed, which are distinguished by closed and open symbols. (B–D) Steady-state values of FabA/FabB ratio (B), total LCMS counts, and fractions of total counts of PlsB and PlsC acyl-ACP substrates (C), and concentrations of fatty acid synthesis pathway enzymes (D) measured two doublings after feeding exogenous fatty acids. For all plots, symbols represent multiple measurements from one culture; line (B) or bars (C) represent average value. For statistical comparison in B, asterisk indicates significant differences between fatty acid feeding conditions and solubilizing carrier control with $P < 0.02$ (Student's *t*-test, 2-tailed unequal distribution performed using Microsoft Excel T.TEST function). For measurements of fatty acid synthesis pathway enzymes at steady state in control culture treated with solubilizing carrier (D), palmitate-fed wild-type culture, and palmitoleic acid-fed culture, three measurements were performed. For *cis*-vaccinate and palmitate-fed Δ *fadD* cultures, two measurements were performed.



synthesis. Our findings advance the field by revealing the mechanism of this inhibition. Specifically, we demonstrate that long-chain acyl-CoA causes long-chain acyl-ACP substrates of phospholipid synthesis to accumulate. This accumulation is a consequence of substrate competition between acyl-ACP and acyl-CoA for acyltransferases PlsB and PlsC. Accumulated long-chain acyl-ACP attenuate malonyl-CoA synthesis by ACC, a well-described inhibitory interaction [25]. We find no evidence that acyl-CoA inhibits FabI *in vivo*. Instead, exogenous fatty acids inhibit fatty acid synthesis via the same feedback mechanism that coordinates fatty acid synthesis with phospholipid synthesis and cell growth. This ensures that fatty acid synthesis is regulated by PlsB activity regardless of the presence of exogenous fatty acids.

We also find that the transcriptional response to exogenous fatty acids is limited to restoring the balance between saturated and unsaturated fatty acid synthesis by tuning FabA and FabB, as the concentrations of all other fatty acid synthesis pathway enzymes remain unchanged. This reflects the requirement for intermediates of the fatty acid synthesis pathway (including the lipopolysaccharide precursor C14:0-OH ACP) and ensures that fatty acid synthesis resumes rapidly when the supply of exogenous fatty acids is exhausted. This design takes advantage of the superior reversibility and responsiveness of post-translational regulation compared to transcription-driven responses [26]. Our finding is important for understanding the potential signaling role of acyl-CoA generated from the breakdown of mislocalized phospholipids in the outer leaflet of the outer membrane [31,37].

We also find that exogenous fatty acids perturb membrane composition not only through direct incorporation, but also by changing the ratio of saturated and unsaturated long-chain acyl-ACP. This amplifies the effects of exogenous fatty acids on membrane composition: palmitate increases the abundance of C16:0 ACP relative to C18:1 ACP, while palmitoleate and *cis*-vacenate increase C18:1 ACP relative to C16:0 ACP. The accumulation of specific acyl-ACP that corresponds to the acyl-CoA produced is a direct consequence of the substrate preferences of PlsB and PlsC. A transcriptional response corrects for this effect by altering the FabA/FabB ratio. The transcriptional regulator FabR binds both C16:0 and C18:1 ACP, with the FabR-C18:1 ACP complex repressing *fabB* transcription and thereby establishing a negative feedback loop that attenuates unsaturated fatty acid synthesis [23]. Previously, the observation that FabR adjusts FabA and FabB expression in response to acyl-CoA led to the proposal that FabR is able to bind both

acyl-ACP and acyl-CoA. However, we find that acyl-CoA directly changes the C16:0/C18:1 ACP ratio due to substrate competition, with saturated acyl-CoA increasing C16:0 ACP and unsaturated acyl-CoA increasing C18:1 ACP. Therefore, it is possible that FabR monitors only the C16:0/C18:1 ACP ratio and does not bind acyl-CoA *in vivo*. A close examination of the data in Zhu *et al.* suggests that FabR exhibits far higher affinity to acyl-ACP than acyl-CoA [23]. *In vitro* competition studies between acyl-CoA and acyl-ACP for triggering DNA binding by FabR could address this question.

Could the substrate competition-driven inhibition of fatty acid synthesis we observe here occur in other bacteria? The enzyme PlsB, which uses both acyl-CoA and acyl-ACP, occurs rarely in bacterial species. Most bacterial species initiate phospholipid synthesis using PlsX and PlsY, which generate LPA in two steps: PlsX converts acyl-ACP to acyl-phosphate, which is subsequently converted to LPA by the G3P acyl transferase PlsY. PlsX and PlsY cannot use acyl-CoA as substrates for the acyltransferase reaction [38]. However, many bacteria use a fatty acid kinase (FakA) to convert exogenous fatty acids to acyl-phosphate [39]. As the reaction catalyzed by PlsX is reversible, acyl-phosphate generated from exogenous fatty acids are converted to acyl-ACP, which can be subsequently fed into the fatty acid synthesis pathway and elongated to long-chain acyl-ACP (Fig. 6). Therefore, as the uptake of fatty acids via FakA and PlsX may also lead to acyl-ACP accumulation, PlsB may not be necessary for exogenous fatty acids to inhibit fatty acid synthesis. The use of acyl-ACP synthases by organisms such as *Chlamydia trachomatis* and *Neisseria gonorrhoeae*, which directly synthesize acyl-ACP from exogenous fatty acids, suggests a more straightforward pathway for generating long-chain acyl-ACP that could inhibit *de novo* fatty acid synthesis [1,40]. Thus, all exogenous fatty acid incorporation pathways characterized to date contribute to a substrate pool that is shared with products of fatty acid synthesis. If feedback inhibition of fatty acid synthesis by long-chain acyl-ACP or acyl-phosphates (at ACC or another step) is also well-conserved, then exogenous fatty acids may inhibit endogenous fatty acid synthesis by substrate competition in many other species. Such a post-translational feedback mechanism would complement transcriptional repression in species that repress *de novo* synthesis in response to exogenous fatty acids. Parallel transcriptional repression and allosteric repression is a recurring motif that has been proposed to ensure robustness and efficiency in biosynthesis pathways [41].

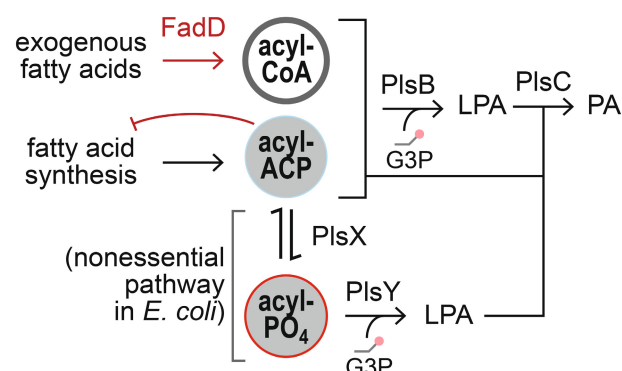
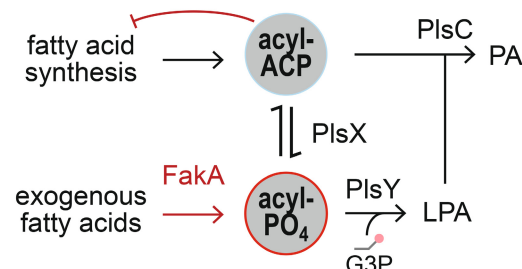
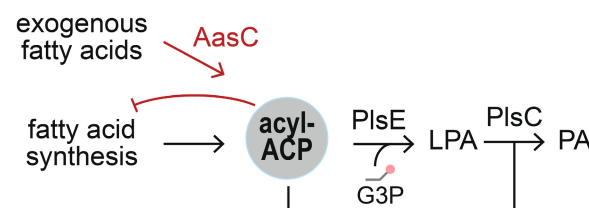
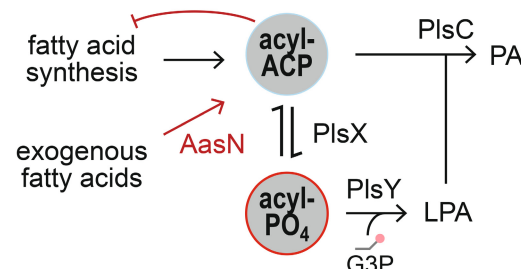
Escherichia coli*:****Gram-positive bacteria:**Chlamydia trachomatis*:*****Neisseria gonorrhoeae*:**

Fig. 6. The conserved intersections of fatty acid synthesis, exogenous fatty acid incorporation, and phospholipid synthesis pathways potentially enable exogenous fatty acids to inhibit *de novo* fatty acid synthesis in diverse bacteria.

The inhibition of fatty acid synthesis by exogenous fatty acids is highly relevant for determining whether an organism can use exogenous fatty acids to evade the effects of fatty acid synthesis-targeting antibiotics. Exogenous fatty acids strongly inhibit malonyl-CoA synthesis by ACC in *Streptococcus pneumoniae*, although the mechanism was not clear [14]. This inhibition is crucial for preserving sufficient holo-ACP despite treatment with FabF and FabI inhibitors (which deplete holo-ACP) to allow exogenous fatty acid incorporation. In contrast, exogenous fatty acids could not sufficiently inhibit malonyl-CoA synthesis by ACC in *Staphylococcus aureus*. As a consequence, treatment with FabF and FabI inhibitors entirely depletes holo-ACP due to continued synthesis of malonyl-ACP (as we observe in *E. coli*). Depletion of holo-ACP prevents exogenous fatty acid incorporation and arrests growth. Investigating how exogenous fatty acids stringently inhibit ACC in *S. pneumoniae* would provide important insight into an antibiotic resistance mechanism.

Acknowledgements

We thank Nicole Scherer for preliminary LCMS analysis and members of the Bokinsky Lab for feedback and

scientific discussions. Project supported by start-up funds to GB from the TU Delft Bionanoscience Department.

Conflict of interest

The authors declare no competing interests.

Author contributions

SvdB: designed and performed experiments, built data analysis pipeline, and evaluated data. FY, AZ-D: LCMS analysis. GB: supervised project, performed pilot experiments, constructed COPASI model, evaluated data, and wrote the manuscript. All authors approved the final manuscript.

Peer review

The peer review history for this article is available at <https://www.webofscience.com/api/gateway/wos/peer-review/10.1002/1873-3468.15092>.

Data accessibility

The COPASI files (.cps) for the model and all source data for figures are available from Figshare at

[10.6084/m9.figshare.27302661](https://doi.org/10.6084/m9.figshare.27302661). The mass spectrometry proteomics data (and acyl-ACP and phospholipids data) have been deposited to the ProteomeXchange Consortium via the PRIDE [45] partner repository with the dataset identifier PXD057199.

References

- Yao J and Rock CO (2017) Exogenous fatty acid metabolism in bacteria. *Biochimie* **141**, 30–39.
- Flegler A, Iswara J, Mänz AT, Schocke FS, Faßbender WA, Hözl G and Lipski A (2022) Exogenous fatty acids affect membrane properties and cold adaptation of *Listeria monocytogenes*. *Sci Rep* **12**, 1499.
- Barbarek SC, Shah R, Paul S, Alvarado G, Appala K, Phillips C, Henderson EC, Strandquist ET, Pokorny A, Singh VK *et al.* (2024) Lipidomics of homeoviscous adaptation to low temperatures in *Staphylococcus aureus* utilizing exogenous straight-chain unsaturated fatty acids. *J Bacteriol* **206**, e0018724.
- Moravec AR, Siv AW, Hobby CR, Lindsay EN, Norbash LV, Shults DJ, Symes SJK and Giles DK (2017) Exogenous polyunsaturated fatty acids impact membrane remodeling and affect virulence phenotypes among pathogenic vibrio species. *Appl Environ Microbiol* **83**, e01415.
- Hobby CR, Herndon JL, Morrow CA, Peters RE, Symes SJK and Giles DK (2019) Exogenous fatty acids alter phospholipid composition, membrane permeability, capacity for biofilm formation, and antimicrobial peptide susceptibility in *Klebsiella pneumoniae*. *Microbiology* **8**, e00635.
- Zhu M, Frank MW, Radka CD, Jeanfavre S, Xu J, Tse MW, Pacheco JA, Kim JS, Pierce K, Deik A *et al.* (2024) Vaginal lactobacillus fatty acid response mechanisms reveal a metabolite-targeted strategy for bacterial vaginosis treatment. *Cell* **187**, 5413–5430.e29.
- Brinster S, Lamberet G, Staels B, Trieu-Cuot P, Gruss A and Poyart C (2009) Type II fatty acid synthesis is not a suitable antibiotic target for gram-positive pathogens. *Nature* **458**, 83–86.
- Silbert DF, Cohen M and Harder ME (1972) The effect of exogenous fatty acids on fatty acid metabolism in *Escherichia coli* K-12. *J Biol Chem* **247**, 1699–1707.
- Silbert DF, Ulbright TM and Honegger JL (1973) Utilization of exogenous fatty acids for complex lipid biosynthesis and its effect on de novo fatty acid formation in *Escherichia coli* K-12. *Biochemistry* **12**, 164–171.
- Lu YJ and Rock CO (2006) Transcriptional regulation of fatty acid biosynthesis in *Streptococcus pneumoniae*. *Mol Microbiol* **59**, 551–566.
- Jerga A and Rock CO (2009) Acyl-acyl carrier protein regulates transcription of fatty acid biosynthetic genes via the FabT repressor in *Streptococcus pneumoniae*. *J Biol Chem* **284**, 15364–15368.
- Zhu L, Zou Q, Cao X and Cronan JE (2019) *Enterococcus faecalis* encodes an atypical auxiliary acyl carrier protein required for efficient regulation of fatty acid synthesis by exogenous fatty acids. *MBio* **10**, e00577.
- Zou Q, Dong H, Zhu L and Cronan JE (2022) The *Enterococcus faecalis* FabT transcription factor regulates fatty acid biosynthesis in response to exogenous fatty acids. *Front Microbiol* **13**, 877582.
- Parsons JB, Frank MW, Subramanian C, Saenkhom P and Rock CO (2011) Metabolic basis for the differential susceptibility of gram-positive pathogens to fatty acid synthesis inhibitors. *Proc Natl Acad Sci U S A* **108**, 15378–15383.
- Radka CD and Rock CO (2022) Mining fatty acid biosynthesis for new antimicrobials. *Annu Rev Microbiol* **76**, 281–304.
- Sinensky M (1974) Homeoviscous adaptation: a homeostatic process that regulates the viscosity of membrane lipids in *Escherichia coli*. *Proc Natl Acad Sci USA* **71**, 522–525.
- Nunn WD and Simons RW (1978) Transport of long-chain fatty acids by *Escherichia coli*: mapping and characterization of mutants in the *fadL* gene. *Proc Natl Acad Sci U S A* **75**, 3377–3381.
- Black PN (1990) Characterization of FadL-specific fatty acid binding in *Escherichia coli*. *Biochim Biophys Acta (BBA)/Lipids Lipid Metab* **1046**, 97–105.
- Kameda K and Nunn W (1981) Purification and characterization of acyl coenzyme A synthetase from *Escherichia coli*. *J Biol Chem* **256**, 5702–5707.
- Polacco ML and Cronan JE (1977) Mechanism of the apparent regulation of *Escherichia coli* unsaturated fatty acid synthesis by exogenous oleic acid. *J Biol Chem* **252**, 5488–5490.
- Xu Y, Heath RJ, Li Z, Rock CO and White SW (2001) The FadR-DNA complex. Transcriptional control of fatty acid metabolism in *Escherichia coli*. *J Biol Chem* **276**, 17373–17379.
- My L, Ghandour Achkar N, Viala JP and Bouveret E (2015) Reassessment of the genetic regulation of fatty acid synthesis in *Escherichia coli*: global positive control by the dual functional regulator FadR. *J Bacteriol* **197**, 1862–1872.
- Zhu K, Zhang YM and Rock CO (2009) Transcriptional regulation of membrane lipid homeostasis in *Escherichia coli*. *J Biol Chem* **284**, 34880–34888.
- Xiao X, Yu X and Khosla C (2013) Metabolic flux between unsaturated and saturated fatty acids is controlled by the FabA:FabB ratio in the fully reconstituted fatty acid biosynthetic pathway of *Escherichia coli*. *Biochemistry* **52**, 8304–8312.

- 25 Davis MS and Cronan J (2001) Inhibition of *Escherichia coli* acetyl coenzyme a carboxylase by acyl-acyl carrier protein. *J Bacteriol* **183**, 1499–1503. doi: [10.1128/JB.183.4.1499-1503.2001](https://doi.org/10.1128/JB.183.4.1499-1503.2001)
- 26 Noga MJ, Büke F, van den Broek NJF, Imholz NCE, Scherer N, Yang F and Bokinsky G (2020) Posttranslational control of PlsB is sufficient to coordinate membrane synthesis with growth in *Escherichia coli*. *MBio* **11**, e02703.
- 27 Garwin JL and Cronan JE (1980) Thermal modulation of fatty acid synthesis in *Escherichia coli* does not involve de novo enzyme synthesis. *J Bacteriol* **141**, 1457–1459.
- 28 Hoogerland L, van den Berg SPH, Suo Y, Moriuchi YW, Zoumaro-Djayoon A, Geurken E, Yang F, Bruggeman F, Burkart MD and Bokinsky G (2024) A temperature-sensitive metabolic valve and a transcriptional feedback loop drive rapid homeoviscous adaptation in *Escherichia coli*. *Nat Commun* **15**, 9386.
- 29 Bergler H, Fuchsbichler S, Högenauer G and Turnowsky F (1996) The enoyl-[acyl-carrier-protein] reductase (FabI) of *Escherichia coli*, which catalyzes a key regulatory step in fatty acid biosynthesis, accepts NADH and NADPH as cofactors and is inhibited by palmitoyl-CoA. *Eur J Biochem* **242**, 689–694.
- 30 Emiola A, Andrews SS, Heller C and George J (2016) Crosstalk between the lipopolysaccharide and phospholipid pathways during outer membrane biogenesis in *Escherichia coli*. *Proc Natl Acad Sci* **113**, 3108–3113.
- 31 May KL and Silhavy TJ (2018) The *Escherichia coli* phospholipase PldA regulates outer membrane homeostasis via lipid signaling. *MBio* **9**, e00379.
- 32 Noga MJ, Cerri M, Imholz N, Tulinski P, Şahin E and Bokinsky G (2016) Mass-spectrometry-based quantification of protein-bound fatty acid synthesis intermediates from *Escherichia coli*. *J Proteome Res* **15**, 3617–3623.
- 33 Heath RJ, Rubin JR, Holland DR, Zhang E, Snow ME and Rock CO (1999) Mechanism of triclosan inhibition of bacterial fatty acid synthesis. *J Biol Chem* **274**, 11110–11114.
- 34 Hoops S, Sahle S, Gauges R, Lee C, Pahle J, Simus N, Singhal M, Xu L, Mendes P and Kummer U (2006) COPASI – a COMplex PATHway SIMulator. *Bioinformatics* **22**, 3067–3074.
- 35 Edwards P, Nelsen JS, Metz JG and Dehesh K (1997) Cloning of the fabF gene in an expression vector and in vitro characterization of recombinant fabF and fabB encoded enzymes from *Escherichia coli*. *FEBS Lett* **402**, 62–66.
- 36 Ruppe S, Mains K and Fox JM (2020) A kinetic rationale for functional redundancy in fatty acid biosynthesis. *Proc Natl Acad Sci USA* **117**, 23557–23564.
- 37 Som N and Reddy M (2023) Cross-talk between phospholipid synthesis and peptidoglycan expansion by a cell wall hydrolase. *Proc Natl Acad Sci USA* **120**, e2300784120.
- 38 Lu YJ, Zhang YM, Grimes KD, Qi J, Lee RE and Rock CO (2006) Acyl-phosphates initiate membrane phospholipid synthesis in gram-positive pathogens. *Mol Cell* **23**, 765–772.
- 39 Parsons JB, Frank MW, Jackson P, Subramanian C and Rock CO (2014) Incorporation of extracellular fatty acids by a fatty acid kinase-dependent pathway in *Staphylococcus aureus*. *Mol Microbiol* **92**, 234–245.
- 40 Yao J, Dodson VJ, Frank MW and Rock CO (2015) Chlamydia trachomatis scavenges host fatty acids for phospholipid synthesis via an acyl-acyl carrier protein synthetase. *J Biol Chem* **290**, 22163–22173.
- 41 Sander T, Farke N, Diehl C, Kuntz M, Glatter T and Link H (2019) Allosteric feedback inhibition enables robust amino acid biosynthesis in *E. coli* by enforcing enzyme overabundance. *Cell Syst* **8**, 66–75.e8.
- 42 Datsenko KA and Wanner BL (2000) One-step inactivation of chromosomal genes in *Escherichia coli* K-12 using PCR products. *Proc Natl Acad Sci USA* **97**, 6640–6645.
- 43 Neidhardt FC, Bloch PL and Smith DF (1974) Culture Medium for Enterobacteria. *J Bacteriol* **119**, 736–747.
- 44 MacLean B, Tomazela DM, Shulman N, Chambers M, Finney GL, Frewen B, Kern R, Tabb DL, Liebler DC and MacCoss MJ (2010) Skyline: an open source document editor for creating and analyzing targeted proteomics experiments. *Bioinformatics* **26**, 966–968.
- 45 Perez-Riverol Y, Bai J, Bandla C, García-Seisdedos D, Hewapathirana S, Kamatchinathan S, Kundu DJ, Prakash A, Frericks-Zipper A, Eisenacher M *et al.* (2022) The PRIDE database resources in 2022: a hub for mass spectrometry-based proteomics evidences. *Nucleic Acids Res* **50**, D543–D552.
- 46 Hughes J and Mellows G (1978) Inhibition of isoleucyl-transfer ribonucleic acid synthetase in *Escherichia coli* by pseudomonic acid. *Biochem J* **176**, 305–318.

Supporting information

Additional supporting information may be found online in the Supporting Information section at the end of the article.

Fig. S1. Phospholipid abundance from initiation of the simulation to the stepwise increase of acyl-CoA at 8000 s.

Table S1. Initial concentrations of species set at non-zero values.

Table S2. Reaction parameters used.